Acta Crystallographica Section F
Structural Biology and Crystallization Communications
ISSN 1744-3091

Crystallization and preliminary diffraction analysis of *Escherichia coli* WrbA in complex with its cofactor flavin mononucleotide

Julie Wolfová,[a,b] Jeroen R. Mesters,[c] Jiří Brynda,[a,d] Rita Grandori,[e] Antonino Natalello,[e] Jannette Carey[f] and Ivana Kutá Smatanová[a,b]*

[a]Institute of Physical Biology, University of South Bohemia České Budějovice, Zámek 136, CZ-373 33 Nové Hrady, Czech Republic, [b]Institute of Systems Biology and Ecology, v.v.i., Academy of Science of the Czech Republic, Zámek 136, CZ-373 33 Nové Hrady, Czech Republic, [c]Institute of Biochemistry, Center for Structural and Cell Biology in Medicine, University of Lübeck, Ratzeburger Allee 160, 23538 Lübeck, Germany, [d]Institute of Molecular Genetics, Academy of Sciences of the Czech Republic, Flemingovo nám. 2, CZ-16637 Prague 6, Czech Republic, [e]Department of Biotechnology and Biosciences, University of Milano-Bicocca, Piazza della Scienza 2, 20126 Milan, Italy, and [f]Chemistry Department, Princeton University, Washington Road and William Street, Princeton, NJ 08544-1009, USA

Correspondence e-mail: ivanaks@seznam.cz

Received 8 March 2007
Accepted 28 May 2007

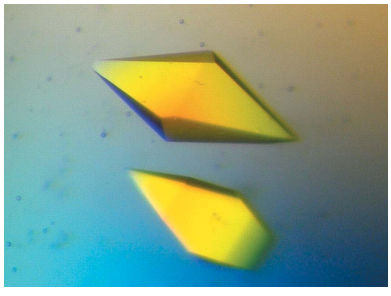

The flavoprotein WrbA from *Escherichia coli* is considered to be the prototype of a new family of multimeric flavodoxin-like proteins that are implicated in cell protection against oxidative stress. The present study is aimed at structural characterization of the *E. coli* protein with respect to its recently revealed oxidoreductase activity. Crystals of WrbA holoprotein in complex with the oxidized flavin cofactor (FMN) were obtained using standard vapour-diffusion techniques. Deep yellow tetragonal crystals obtained from differing crystallization conditions display different space groups and unit-cell parameters. X-ray crystal structures of the WrbA holoprotein have been determined to resolutions of 2.0 and 2.6 Å.

1. Introduction

The protein WrbA from *Escherichia coli* is the founding member of a family of flavodoxin-like proteins that are suggested by homology to participate in cellular defence against oxidative stress (Grandori & Carey, 1994). The designation of the *E. coli* WrbA protein as tryptophan-repressor binding protein A refers to its discovery: it was copurified with the tryptophan-repressor protein TrpR and reported to enhance the stability of DNA binding by TrpR (Yang *et al.*, 1993). However, this role was put under question by the finding that WrbA exerted no specific effect on TrpR–DNA binding (Grandori *et al.*, 1998). This work also showed that WrbA binds flavin mononucleotide (FMN) more weakly than the flavodoxins, but that it nevertheless does so specifically, and that it undergoes dimer–tetramer equilibrium in solution. Sequence similarity with NAD(P)H:quinone oxidoreductases suggested that the WrbA family might share this function (Laskowski *et al.*, 2002; Daher *et al.*, 2005). Recently, Patridge & Ferry (2006) reported that *E. coli* WrbA and its homologue from *Archaeoglobus fulgidus* display quinone oxidoreductase activity, with FMN as the redox-active cofactor and NADH as the preferred electron donor. Enzymes with NAD(P)H:quinone reductase activity are proposed to maintain quinones in a fully reduced state in order to protect cells against deleterious reactive oxygen species from one-electron redox cycling (Jensen *et al.*, 2002; Cohen *et al.*, 2004; Jaiswal, 2000; Morre, 2004; Wang *et al.*, 2006; Gonzalez *et al.*, 2005; Talalay & Dinkova-Kostova, 2004; Bianchet *et al.*, 2004; Ross & Siegel, 2004). Consistent with this role, *E. coli* WrbA transfers two electrons at a time and does not stabilize a flavin semiquinone intermediate (Nöll *et al.*, 2006). Transcription of *E. coli* WrbA is controlled by the stress response factor *rpoS* (Lacour & Landini, 2004). A wide range of external stressors such as acids or H_2O_2 have been reported to induce WrbA expression (Chang *et al.*, 2002; Tucker *et al.*, 2002; Kang *et al.*, 2005). These results implicate the WrbA family in the protection of cells against oxidative stress.

The crystal structures of WrbA homologues from *Deinococcus radiodurans* (37% sequence identity with *E. coli* WrbA) and *Pseudomonas aeruginosa* (40% sequence identity with *E. coli* WrbA) have been published (Gorman & Shapiro, 2005). These structures confirm that the members of the WrbA family adopt an α/β twisted open-sheet fold typical of flavodoxins and form homotetramers that bind one FMN molecule per monomer. However, the structures did not clarify why WrbA proteins function as tetramers or why they bind

FMN specifically but only weakly. Furthermore, the only high-resolution structure to be reported is that of the *D. radiodurans* apoprotein; the holoprotein form is of much lower resolution and both the forms of the *P. aeruginosa* protein are poorly ordered, with many missing chain segments. *D. radiodurans* is a eubacterial extremophile and its WrbA structure may reflect adaptations of sequence and structure required for radiation stability. This fact, together with its relatively low sequence identity to *E. coli* WrbA, limits the structural interpretation of the biochemical data, which are available only for the *E. coli* WrbA protein. For these reasons, we have been pursuing the crystallization of *E. coli* WrbA. We have previously reported the crystallization of *E. coli* WrbA apoprotein (Wolfova *et al.*, 2005). Here, we report the crystallization and preliminary diffraction analysis of *E. coli* WrbA in complex with its FMN cofactor.

2. Materials and methods

2.1. Expression, purification and holoprotein reconstitution

Recombinant WrbA protein was expressed in *E. coli* CY15071(λDE3) cells and purified using DEAE-cellulose (DEAE Highprep, Pharmacia) and Affi-Gel Blue (Bio-Rad) affinity column chromatography, as previously described by Grandori *et al.* (1998) and Natalello *et al.* (2007). The purity and monomer molecular weight (about 21 kDa) were determined by electrospray-ionization mass spectrometry (ESI–MS) and by SDS–PAGE performed according to Laemmli (1970) in a Bio-Rad minigel apparatus using 12% Tris–glycine gels stained with Coomassie Blue R250. The final concentration of the purified protein was determined by UV absorption spectroscopy (Spectronic Unicam UV 300, Cambridge, England) using the previously reported extinction coefficient of 22 831 M^{-1} cm^{-1} at 280 nm (Grandori *et al.*, 1998). Pure WrbA protein was obtained without bound cofactor owing to loss of FMN during affinity chromatography. The holoprotein for crystallization was prepared by incubating 0.25 m*M* pure WrbA apoprotein with 0.25 m*M* FMN (Sigma), affording 96% occupancy of the FMN–WrbA complex according to the equilibrium constant of 2 μ*M* as determined by Grandori *et al.* (1998). The use of an excess of cofactor over WrbA protein for reconstitution was prohibited owing to precipitation of free FMN, which prevented the protein from crystallizing (data not shown). The reconstituted WrbA holoprotein is in the oxidized form as shown by the absorption spectra (Grandori *et al.*, 1998), which are typical of oxidized flavoproteins (Mayhew & Massey, 1969; Mayhew & Tollin, 1992).

2.2. Crystallization

Reconstituted WrbA holoprotein at 0.25 m*M* (5 mg ml^{-1}) in 20 m*M* Tris–HCl pH 7.5 was used for the crystallization trials. As a starting point, the crystallization conditions found previously for WrbA apoprotein were tested (reservoir containing 2.0 *M* ammonium sulfate in 0.1 *M* Tris–HCl pH 8.5; Wolfova *et al.*, 2005). Screening of varying temperatures (ranging from 277 to 298 K) and concentrations of ammonium sulfate (1.5–2.6 *M* at pH values ranging from 7.0 to 9.0) was carried out using the sitting-drop vapour-diffusion technique. Crystallization trials using droplets containing equal volumes of protein and precipitant solution were performed in Cryschem plates (Hampton Research, Aliso Viejo, CA, USA). In addition, 0.5–2.0 m*M* cadmium chloride and 1.0 m*M* lithium citrate were tested as additives because of their positive effect on WrbA apoprotein crystallization (Wolfova *et al.*, 2005). Commercially available crystal screening kits (Hampton Research Crystal Screen Kit, Sigma Basic and Extension Crystallization Kits for Proteins) were also used for crystallization trials; screening was carried out using 96-well Intelliplates and the Phoenix microdispenser (Art Robbins Instruments).

2.3. Data collection and processing

Diffraction data for WrbA holoprotein crystals were collected using synchrotron radiation at the Joint University of Hamburg/IMB Jena/EMBL beamline X13 (wavelength 0.804 Å), Deutsches Elektronen-Synchrotron (DESY, Hamburg), which is equipped with a MAR CCD detector (X-ray Research). Crystals grown from the conditions reported here were mounted directly into cryoloops without additional cryoprotection and flash-frozen in a stream of nitrogen gas (Oxford Cryosystems) at 100 K. The addition of cryoprotectant was not required since the crystals were obtained at high polyethylene glycol concentrations. X-ray data were recorded to a Bragg spacing of 2.6 Å for crystals grown from 25% ethylene glycol (crystal form I) and to 2.0 Å for crystals grown from 20% PEG 8000 in 0.1 *M* Tris–HCl pH 8.0 or 30% PEG 4000 in 0.1 *M* Tris–HCl pH 8.5, 0.2 *M* $MgCl_2$ (crystal form II). The programs *DENZO* and *SCALEPACK* (Otwinowski & Minor, 1997) were used for processing, indexing and scaling of the data.

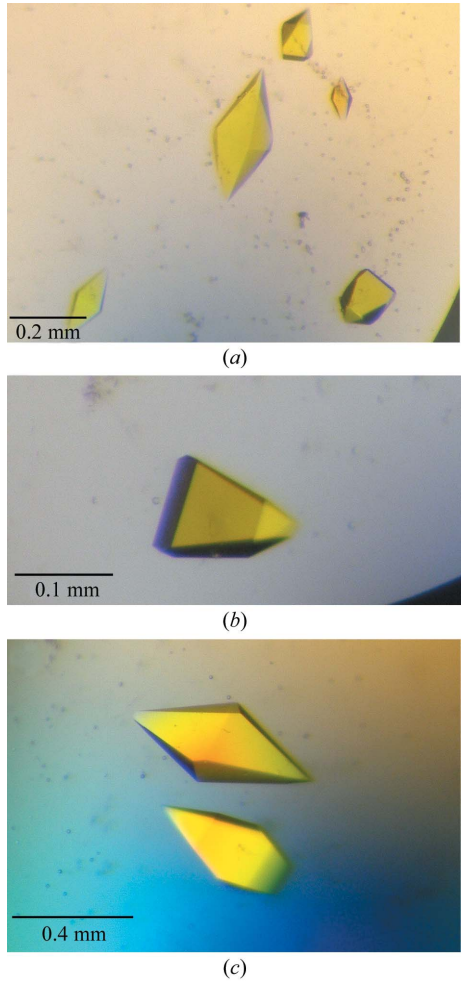

Figure 1
WrbA holoprotein crystals grown by the sitting-drop vapour-diffusion method from reservoirs containing: (*a*) 25% ethylene glycol (crystal form I), (*b*) 20% PEG 8000, 0.1 *M* Tris–HCl pH 8.0 (crystal form II), (*c*) 30% PEG 4000, 0.1 *M* Tris–HCl pH 8.5, 0.2 *M* $MgCl_2$.

Table 1
Data-collection statistics for WrbA holoprotein crystals.

Values in parentheses are for the highest resolution shell.

	WrbA–FMN†	WrbA–FMN‡
Space group	$P4_32_12$	$P4_12_12$
Crystal system	Primitive tetragonal	Primitive tetragonal
Unit-cell parameters (Å)	$a = b = 94.35$, $c = 175.38$	$a = b = 61.13$, $c = 168.38$
Resolution range (Å)	35.0–2.6 (2.69–2.60)	35.0–2.0 (2.04–1.99)
Solvent content (%)	73	34
No. of collected images	180	270
Oscillation angle (°)	1	1
No. of measured reflections	179066	142741
No. of unique reflections	24986	20763
Redundancy	7.2 (6.7)	6.9 (6.5)
Completeness (%)	98.9 (98.1)	90.8 (84.1)
$R_{\rm merge}$§	0.14 (0.62)	0.09 (0.51)
$\langle I/\sigma(I)\rangle$	12.35 (2.64)	16.94 (3.42)
Mosaicity (°)	0.38	0.84
No. of molecules per ASU	2	2

† WrbA holoprotein crystal form I grown from 25% ethylene glycol. ‡ WrbA holoprotein crystal form II grown from 20% PEG 8000, 0.1 *M* Tris–HCl pH 8.0. Similar data were obtained for crystals grown from 30% PEG 4000, 0.1 *M* Tris–HCl pH 8.5, 0.2 *M* $MgCl_2$ (data not shown). § $R_{\rm merge} = \sum|I - \langle I\rangle|/\sum\langle I\rangle$, where I is an individual intensity measurement and $\langle I\rangle$ is the average intensity for this reflection. The value of $R_{\rm merge}$ was calculated by summation over all data.

2.4. Preliminary structure solution

The structure of crystal form I (space group $P4_32_12$, diffracting to 2.6 Å; Table 1) was solved by molecular-replacement techniques using *P. aeruginosa* WrbA holoprotein as the template (PDB ID code 1zwl; Gorman & Shapiro, 2005). The structure of crystal form II (space group $P4_12_12$, diffracting to 2.0 Å; Table 1) was solved using a partially refined structure of the first crystal form as a search model for molecular replacement. Self- and cross-rotation functions, translational searches and rigid-body refinement were performed using the programs *AMoRe* (Navaza, 2001) and *MOLREP* (Vagin & Teplyakov, 2000) as implemented in the *CCP*4 suite (Collaborative Computational Project, Number 4, 1994).

3. Results and discussion

3.1. Crystallization and diffraction data

Crystallization conditions based on those found for WrbA apoprotein (Wolfova *et al.*, 2005) were tested for WrbA holoprotein. However, these conditions yielded no crystals of WrbA holoprotein. Therefore, further screening was carried out using standard crystallization screening kits in 96-well sitting-drop vapour-diffusion experiments at different temperatures. After two weeks, well formed tetragonal crystals grew at 285 K from three different conditions (25% ethylene glycol; 20% PEG 8000, 0.1 *M* Tris–HCl pH 8.0; 30% PEG 4000, 0.1 *M* Tris–HCl pH 8.5, 0.2 *M* $MgCl_2$). The crystals reached maximum dimensions of 0.48 × 0.2 × 0.2 mm and were deep yellow in colour, indicating that the FMN cofactor is present in its oxidized form (Fig. 1). Thus, the flavin cofactor in the crystals retained the redox state observed by absorption spectroscopy after holoprotein reconstitution (Grandori *et al.*, 1998). The holoprotein crystals grown under the conditions reported here required no additional optimization steps to yield high-quality diffraction data. In contrast, crystallization of WrbA apoprotein required the use of additives and gels to reduce formation of multicrystalline clusters (Wolfova *et al.*, 2005). Although optimization yielded single crystals, the apoprotein structure could not be solved owing to high crystal mosaicity and anisotropy.

Diffraction data collected from holoprotein crystals obtained under different crystallization conditions revealed two forms of primitive tetragonal crystals (see §3.2) that differed in space group and unit-cell parameters. The data-collection statistics are presented in Table 1. Crystals grown from the two conditions containing PEG provided similar diffraction data; hence, only data for the crystals grown from 20% PEG 8000, 0.1 *M* Tris–HCl pH 8.0 are presented. The crystals grown from 25% ethylene glycol belong to space group $P4_32_12$, with unit-cell parameters $a = b = 94.35$, $c = 175.38$ Å. The crystals grown from 20% PEG 8000 belong to space group $P4_12_12$, with unit-cell parameters $a = b = 61.13$, $c = 168.38$ Å. The resolution of the diffraction data obtainable with these two crystal forms is also rather different: 2.6 and 2.0 Å, respectively. The very different unit cells of the two crystal forms yield correspondingly large differences in the crystal volume per unit of molecular weight, $V_{\rm M}$, which is 4.6 and 1.85 Å^3 Da^{-1}, respectively. These values correspond to solvent contents of 73% and 34% (Matthews, 1968). The low protein content explains the lower resolution of the data obtained from the crystals grown from 25% ethylene glycol. The diffraction limit of the crystals grown from PEG 8000 represents the best resolution reported to date for WrbA holoprotein.

3.2. Structure solution of the WrbA–FMN complexes

3.2.1. Structure solution of crystal form I grown from 25% ethylene glycol. Inspection of axial reflections indicates one fourfold screw, one twofold screw and one twofold axis, suggesting either space group $P4_12_12$ or $P4_32_12$. Fig. 2 shows the stereographic projection of the $\kappa = 180^\circ$ section of the self-rotation function for this crystal form. The crystallographic $P422$ symmetry corresponds to the peak at the centre and peaks at the edge of this projection. The noncrystallographic twofold symmetry follows from the four equivalent peaks around the central peak on this section. The correct space group $P4_32_12$ was deduced from a comparison of solutions from

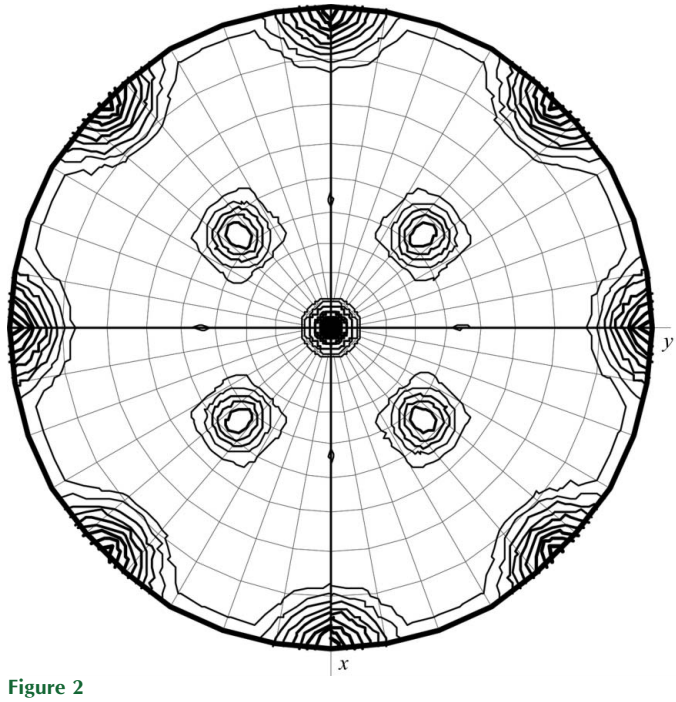

Figure 2
Stereographic projection of the $\kappa = 180^\circ$ section of the self-rotation function calculated using data for $P4_32_12$ crystals (crystal form I) in the range 40.0–4.0 Å and an integration radius of 20 Å.

the translation function for the enantiomorphic space groups. Using a monomer of *P. aeruginosa* holoprotein (PDB code 1zwl; monomer plus bound FMN but without water molecules) as the search model in molecular replacement, a dimer was identified consisting of the two best monomer solutions obtained (dimer solution, R = 48.6%, CC = 44.2%; first incorrect solution, R = 52.3%, CC = 28.6%). After rigid-body refinement (*REFMAC*5; Murshudov *et al.*, 1997), the initial R factor of 47.8% fell to 39.7% ($R_{\rm free}$ = 42.7%) in the very first cycles of refinement and rebuilding. The asymmetric part of the unit cell contains two chemically identical molecules that form a tetramer with a symmetry-related dimer. The tetramer assembles as a dimer of dimers of 222 symmetry with the twofold axes (noncrystallographic) oriented diagonally to the crystallographic axes; this is also nicely visible from the stereographic projection of the self-rotation function (Fig. 2).

3.2.2. Structure solution of crystal form II grown from 20% PEG 8000. Inspection of axial reflections implies one fourfold screw, one twofold screw and one twofold axis. The correct space group $P4_12_12$ was deduced from a comparison of solutions from the translation function for the enantiomorphic space groups ($P4_12_12$/$P4_32_12$ with CC = 62.5%/34.3%). In this case, the structure of crystal form I was used as a search model in molecular replacement. Again, a dimer was identified consisting of the two best monomer solutions (dimer solution, R = 40.2%, CC = 62.5%; first incorrect solution, R = 40.5%, CC = 61.8%). This solution was further improved by rigid-body refinement (*MOLREP*; R = 38.7%, CC = 65.0%). This dimer also forms a tetramer, *i.e.* a dimer of dimers with 222 symmetry. However, the noncrystallographic twofold axes are oriented differently compared with crystal form I.

3.3. Preliminary analysis of crystal packing

Preliminary analysis of the diffraction data provided an approximate view of the structural models. The asymmetric unit of both crystal forms contains a dimer that forms a compact tetramer with two adjacent monomers, which is consistent with evidence that *E. coli* WrbA undergoes a dimer–tetramer equilibrium in solution (Grandori *et al.*, 1998). Fourier-transform infrared spectroscopy suggests a reduction of conformational heterogeneity and/or dynamics of WrbA upon FMN binding and mass spectroscopy reveals that FMN binding favours tetramer formation from WrbA dimers while not affecting the monomer–dimer distribution (Natalello *et al.*, 2007). FMN is also proposed to favour tetramer formation by WrbA homologues (Gorman & Shapiro, 2005).

Ligand binding is among various factors that affect protein crystallization, as summarized by Ducruix & Giegé (1999). Here, FMN is suggested to influence the crystallization of WrbA through specific binding leading to favourable intermolecular interactions and/or by reducing the conformational heterogeneity of the protein originating from dynamics of secondary, tertiary or quaternary structure or from aggregation. For the structures reported here, the bound FMN cofactor appears to affect a nearby surface-exposed mobile helix and loop involved in crystal lattice formation (see Fig. 3). Through specific interactions with WrbA, FMN apparently restricts the conformational degrees of freedom of this part of the chain so that chain excursions and/or species distributions are reduced. Notably, FMN protects WrbA against deliberate proteolysis, resulting in a longer persistence of the holoprotein than the apoprotein (Wolfova & Carey, unpublished observations). Thus, the holoprotein crystals reported here differ fundamentally from those used in the previously reported structures, in which FMN was soaked into crystals of apoprotein (Gorman & Shapiro, 2005).

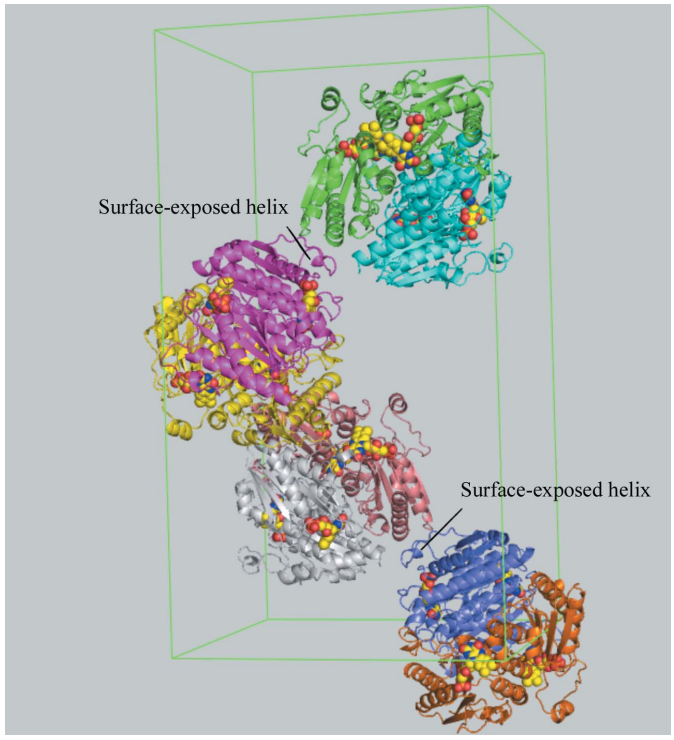

Figure 3
Crystal packing of the WrbA holoprotein in crystal form I grown from 25% ethylene glycol. Each dimer is uniquely coloured. FMN is shown in space-filling representation and the surface-exposed helix discussed in the text is indicated.

The entire polypeptide chain appears to be resolved in the 2.6 Å resolution structure. Thus, for the first time all loops are fully visible in the electron-density maps. In contrast, a few disordered parts are present in the high-resolution model. Consequently, in order to obtain maximum structural information, both structural models will have to be pursued. The two structures are currently in the process of being refined and interpreted in detail.

The authors thank Rolf Hilgenfeld (University of Luebeck) and Juraj Sedláček (Academy of Sciences of the Czech Republic, Prague) for their generous support, and Rüdiger Ettrich for his advice and comments. This work is supported by the Ministry of Education of the Czech Republic (projects Kontakt ME640, MSM6007665808 and LC06010), by the Academy of Sciences of the Czech Republic (AV0Z60870520) and by NSF INT 03-09049 to JC. Diffraction measurements at the Deutsches Elektronen-Synchrotron (DESY, Hamburg) were supported by the European Community, Research Infrastructure Action under the FP6 'Structuring the European Research Area Specific Programme' to the EMBL Hamburg Outstation, contract No. RII3-CT-2004-506008.

References

Bianchet, M. A., Faig, M. & Amzel, L. M. (2004). *Methods Enzymol.* **382**, 144–174.
Chang, D. E., Smalley, D. J. & Conway, T. (2002). *Mol. Microbiol.* **45**, 289–306.
Cohen, R., Suzuki, M. R. & Hammel, K. E. (2004). *Appl. Environ. Microbiol.* **70**, 324–331.
Collaborative Computational Project, Number 4 (1994). *Acta Cryst.* D**50**, 760–763.
Daher, B. S., Venancio, E. J., de Freitas, S. M., Bao, S. N., Vianney, P. V., Andrade, R. V., Dantas, A. S., Soares, C. M., Silva-Pereira, I. & Felipe, M. S. (2005). *Fungal Genet. Biol.* **42**, 434–443.

Ducruix, A. & Giegé, R. (1999). *Crystallization of Nucleic Acids and Proteins: A Practical Approach*, 2nd ed. Oxford University Press.
Gonzalez, C. F., Ackerley, D. F., Lynch, S. V. & Matin, A. (2005). *J. Biol. Chem.* **280**, 22590–22595.
Gorman, J. & Shapiro, L. (2005). *Protein Sci.* **14**, 3004–3012.
Grandori, R. & Carey, J. (1994). *Protein Sci.* **3**, 2185–2193.
Grandori, R., Khalifah, P., Boice, J. A., Fairman, R., Giovanelli, K. & Carey, J. (1998). *J. Biol. Chem.* **273**, 20960–20966.
Jaiswal, A. K. (2000). *Free Radic. Biol. Med.* **29**, 254–262.
Jensen, K. A. Jr, Ryan, Z. C., Vanden Wymelenberg, A., Cullen, D. & Hammel, K. E. (2002). *Appl. Environ. Microbiol.* **68**, 2699–2703.
Kang, Y., Weber, K. D., Qiu, Y., Kiley, P. J. & Blattner, F. R. (2005). *J. Bacteriol.* **187**, 1135–1160.
Lacour, S. & Landini, P. (2004). *J. Bacteriol.* **186**, 7186–7195.
Laemmli, U. K. (1970). *Nature (London)*, **227**, 680–685.
Laskowski, M. J., Dreher, K. A., Gehring, M. A., Abel, S., Gensler, A. L. & Sussex, I. M. (2002). *Plant Physiol.* **128**, 578–590.
Matthews, B. W. (1968). *J. Mol. Biol.* **33**, 491–497.
Mayhew, S. G. & Massey, V. (1969). *J. Biol. Chem.* **244**, 794–802.
Mayhew, S. G. & Tollin, G. (1992). *Chemistry and Biochemistry of Flavoenzymes*, Vol. 3, edited by F. Mueller, pp. 389–426. Boca Raton: CRC Press.
Morre, D. J. (2004). *Methods Enzymol.* **378**, 179–199.
Murshudov, G. N., Vagin, A. A. & Dodson, E. J. (1997). *Acta Cryst.* D**53**, 240–255.
Natalello, A., Doglia, S. M., Carey, J. & Grandori, R. (2007). *Biochemistry*, **46**, 543–553.
Navaza, J. (2001). *Acta Cryst.* D**57**, 1367–1372.
Nöll, G., Kozma, E., Grandori, R., Carey, J., Schödl, T., Hauska, G. & Daub, J. (2006). *Langmuir*, **22**, 2378–2383.
Otwinowski, Z. & Minor, W. (1997). *Methods Enzymol.* **276**, 307–326.
Patridge, E. V. & Ferry, J. G. (2006). *J. Bacteriol.* **188**, 3498–3506.
Ross, D. & Siegel, D. (2004). *Methods Enzymol.* **382**, 115–144.
Talalay, P. & Dinkova-Kostova, A. T. (2004). *Methods Enzymol.* **382**, 355–364.
Tucker, D. L., Tucker, N. & Conway, T. (2002). *J. Bacteriol.* **184**, 6551–6558.
Vagin, A. & Teplyakov, A. (2000). *Acta Cryst.* D**56**, 1622–1624.
Wang, G., Alamuri, P. & Maier, R. J. (2006). *Mol. Microbiol.* **61**, 847–860.
Wolfova, J., Grandori, R., Kozma, E., Chatterjee, N., Carey, J. & Kuta Smatanova, I. (2005). *J. Cryst. Growth*, **284**, 502–505.
Yang, W., Ni, L. & Somerville, R. L. (1993). *Proc. Natl Acad. Sci. USA*, **90**, 5796–5800.